

CAAP Quarterly Report

Date of Report: *April 7th, 2020*

Contract Number: *693JK318500010CAAP*

Prepared for: *U.S. DOT Pipeline and Hazardous Materials Safety Administration*

Project Title: *Brain-Inspired Learning Framework to Bridging Information, Uncertainty and Human-Machine Decision-Making for Decoding Variance in Pipeline Computational Models*

Prepared by: *North Dakota State University*

Contact Information: *Ms. Zi Zhang, PhD student, Email: zi.zhang@ndsu.edu, Phone: 701-231-7204; Dr. Hong Pan, Postdoc, Email: hong.pan@ndsu.edu; Mr. Matthew Pearson, M.S. student, Email: matthew.pearson@ndsu.edu, Phone: 701-231-7204; Dr. Zhibin Lin, Email: zhibin.lin@ndsu.edu, Phone: 717-231-7204*

For quarterly period ending: *April 7th, 2020*

Business and Activity Section

(a) Generated Commitments

Top journal paper published: a journal paper, entitled “*Machine learning-enriched Lamb wave approaches for automated damage detection*” was published in a top Journal - *Nanomaterials* (Impact factor=3.031). PhD student Zi Zhang who mainly takes charge of this research was the first author.

Conference paper accepted under virtual presentation duo to Covid-19 situation: two conference papers, entitled “*Corrosion-induced damage detection and conditional assessment for metallic civil structures using machine learning approaches*” and “*Conditional assessment of large-scale infrastructure systems using deep learning approaches*”, were accepted as conference papers and presentation under virtual presentation duo to Covid-19 situation, *2020 SPIE Smart Structures and Nondestructive Evaluation, April 26-30, Anaheim, California, USA.*

(b) Status Update of Past Quarter Activities

The research activities in the 6th quarter included: (i) Continuing efforts by decoding variance experienced from material and structural integrity in **Task 2**; and (ii) Modeling and decoding variance experienced from structural uncertainties in **Task 4**, as summarized in Section (d).

(c) Cost share activity

Cost share was from the graduate students' tuition waiver.

(d) Summary of detailed work for Tasks 2, and 4

Tasks 2 and 4: Summary of continuing efforts by decoding variance experienced from material and structural integrity, and modeling and decoding variance experienced from structural uncertainties.

6.1 Objectives in the 6th Quarter

Large-scale networked on shore gas and liquid transmission pipelines are susceptible to degradation, corrosion and damages due to aging, loads and man-made disasters. Therefore, understanding of characteristics and performance, including detecting various mechanical damages, for these pipelines in-service operation is needed to provide timely recommendations for maintenance and other precautions measures to avoid costly disasters.

Thus, this study aimed to develop a new deep learning-based framework for decoding variances associated with mechanical damage and structural uncertainty.

6.2 Data generated from computer modeling of guided wave through oil/gas pipelines

6.2.1 Dispersion curves along pipeline

Three main modes were generated when guided wave propagated along a hollow cylindrical pipe, including longitudinal mode (L mode) torsional mode (T mode) and flexural mode (F mode). The previous researches proved that the longitudinal $L(0,2)$ mode achieves all pipe wall coverage because of the axisymmetric characteristics. According to **Fig. 1**, $L(0,2)$ mode in range 50 to 150 kHz has smaller dispersion, higher speed and lower distorted mode, which is commonly used in testing.

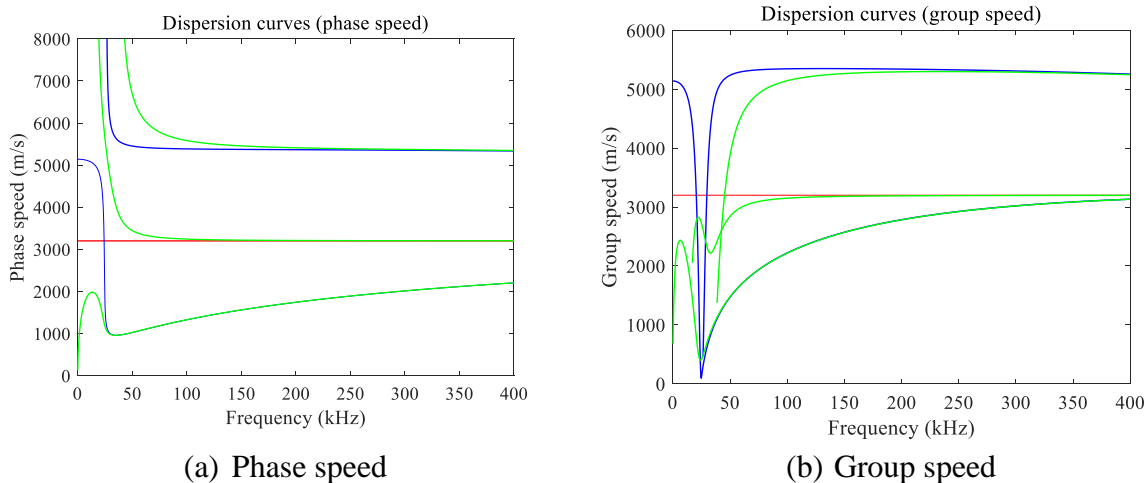


Fig. 1 Multiple mode of guided wave along a pipeline

6.2.2 Numerical simulation for pipeline

Oil/gas pipeline was simulated using 3D FE modeling through COMSOL. The prototype of a steel pipeline was selected from the literature [10], where its dimension is 76-mm in outside diameter and 4 mm in wall thickness, and with a length of 1500 mm. As shown in **Fig. 2**, the excitation signal with 100kHz, $D(t)$, was defined by a 5-cycle sine function operated with a Hanning window by the form:

$$D(t) = A(1 - \cos \frac{2\pi f_c t}{n}) \sin(2\pi f_c t) \quad (1)$$

where A is amplitude of the signal, f_c is the frequency and n is the number of the period. This kind of axial loading pattern can generate a single guided wave in L(0,2) mode propagated in the pipe. The signal was defined in COMSOL to simulate the effect of the actuator, while the displacement was set at the one side.

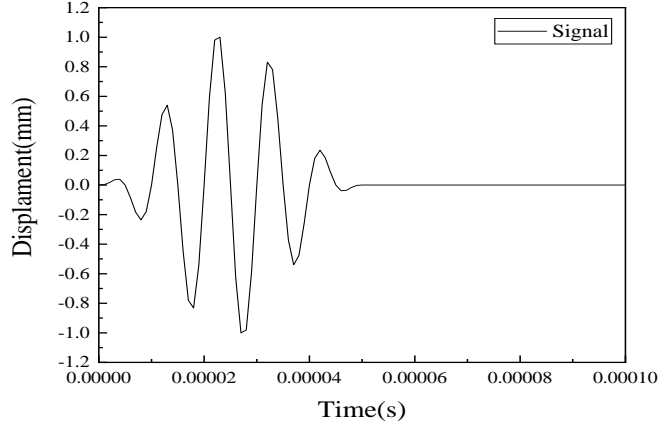


Fig. 2 Excitation signal

6.2.3 Design of Scenarios and Data Augmentation

Four different scenarios were set in this research, including undamaged state, undamaged pipe with weldment state, notch-shaped damage without weldment state and notch-shaped damage with weldment state. To consider the uncertainty happened in actual situation, noise was added to the collected signals based on the signal to noise ratio (SNR) that represents the ratio of the signal strength to the background noise strength as:

$$SNR_{dB} = 10 \log_{10} \left(\frac{P_{\text{signal}}}{P_{\text{noise}}} \right) \quad (2)$$

where P_{signal} and P_{noise} are the average power of signal and noise by the dB scale, respectively. Six different noise levels, ranging from 60 dB to 120 dB, were selected to State # 1-4 for machine learning to check the sensitivity of the uncertainty due to noise.

6.3 Data fusion

6.3.1 Continuous wavelet transforms

Guided wave exhibits non-stationary and nonlinear behavior. Time domain/frequency/time-frequency analyses are effective to track the change of a system and its nonlinear behavior. The continuous wavelet transform (CWT) decomposes the signal into a time-frequency domain for analyzing nonstationary signals by scaling and shifting the basis wavelet. In this study, the multi-resolution wavelet analysis has been used to decompose the signal in time and frequency domain, while the continuous wavelet transforms of a continuous signal, $x(t)$, is defined by:

$$Wx(a, b) = x \otimes \psi_{b,a}(t) = \frac{1}{\sqrt{a}} \int_{-\infty}^{+\infty} x(t) \psi^* \left(\frac{t-b}{a} \right) dt \quad (3)$$

where ψ and ψ^* are the basic function and its complex conjugate; a and b are the scale and translation factors, respectively. Eqn. (1) is to decompose $x(t)$ into basic function $\Psi((t-b)/a)\Psi\left(\frac{t-b}{a}\right)$, named the mother wavelet. The scale factor a is equal to 2. The frequency spectrum of the wavelet is stretched by a factor of 2 and all frequency components shift up by a factor of 2. The discrete wavelet transform can be treated as a band-pass filter:

$$Wx(j, k) = \int_{-\infty}^{+\infty} x(t)2^{\frac{j}{2}}\psi^*(2^j t - k)dt \quad (4)$$

Fig. 3 represented the time-frequency images of the signals under different noise level by CWT. The images were clear with the SNRs = 120 dB and 100 dB. As the noise level increased to 80 dB, the main feature part at the bottom was still existed, though some irregular texture was distributed in the image. While when noise level reached to 60 dB, the image showed the texture without the yellow part, suggesting that the noise interference significantly affected the original pattern of data.

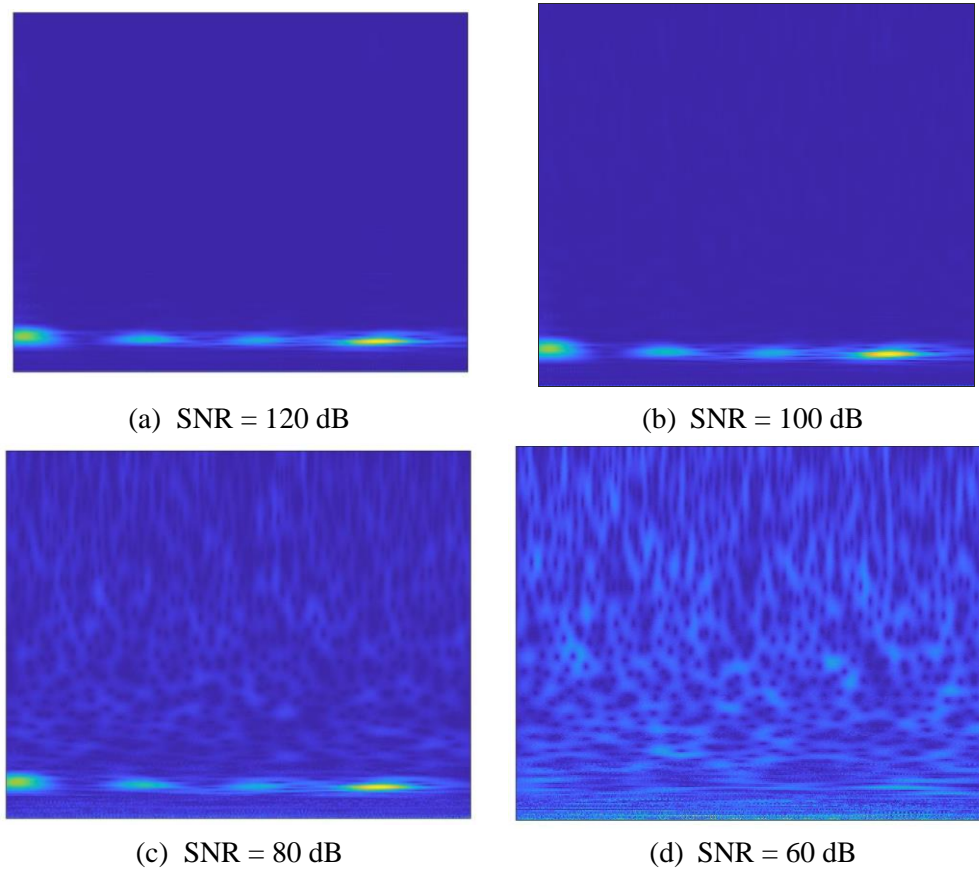
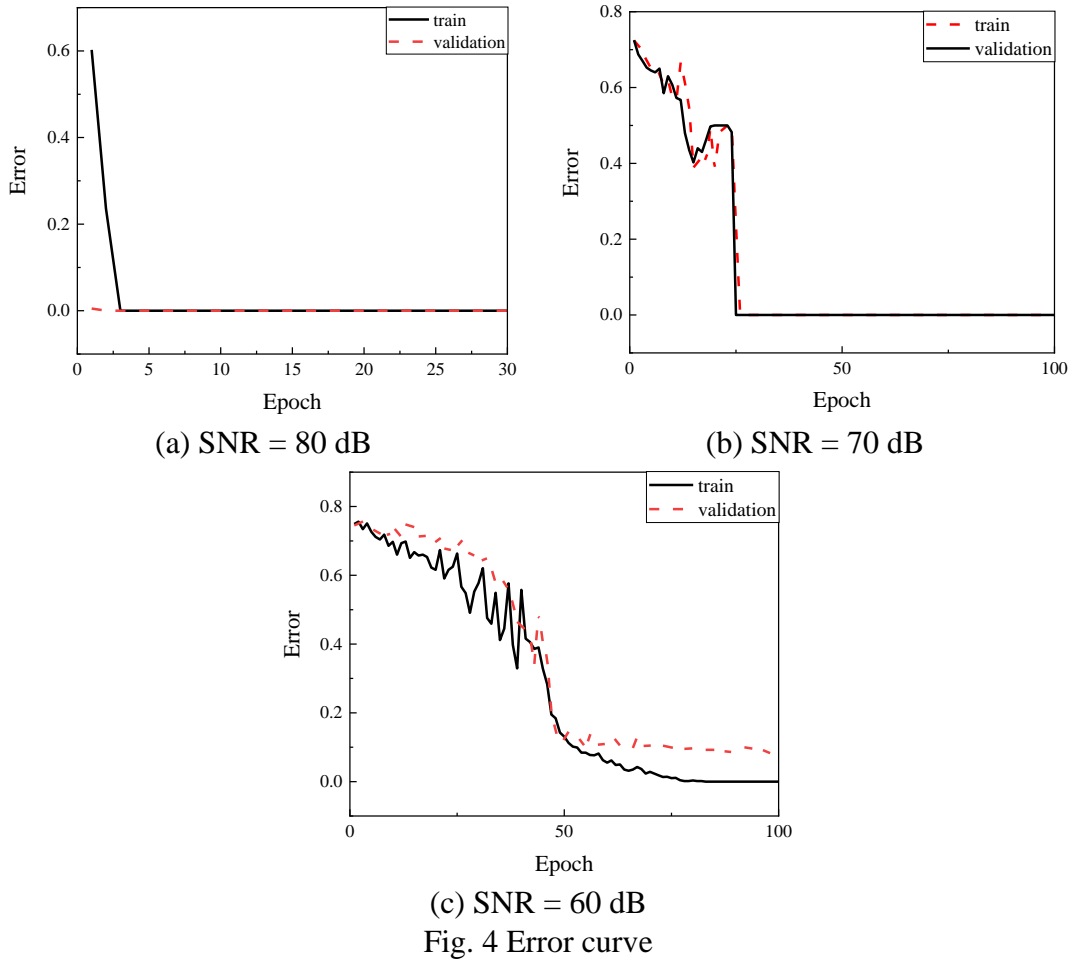


Fig. 3 Time-frequency images of signals under different noise levels

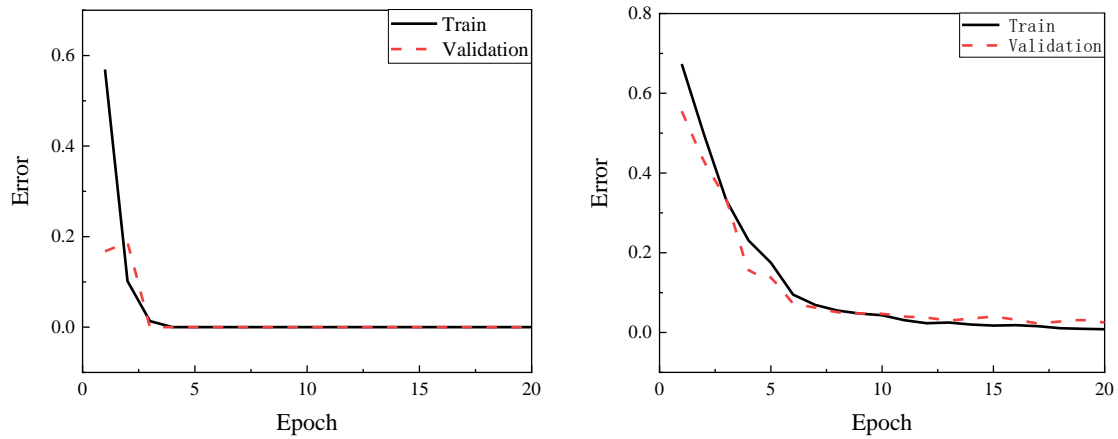
6.3.2 CNN model training and validation

To build the convolutional neural network, 2000 sample data was involved in this system, including 60% of it for training, 20% of the data for validation and the rest for testing. The results of the first network trained by time series signals were shown in **Fig. 4** representing the 80 dB, 70 dB and 60 dB respectively. With the SNR reduced, the error curves of train and validation were slowly converged to zero. Under low noise level, the characteristics between different classes were easy to be trained so that only the network only used 2 epochs to get the 100% prediction. When the noise level equals to 70 dB, the accuracy of the prediction was equal to 100% after 25 epochs' training. The situation became terrible when SNR = 60 dB. After 100 epochs training, the error rate of the training data was 0, and the error of

the validation was about 0.1, which means the accuracy of the prediction was lower. However, the result could not prove that the network was bad. Because under this noise level, the signals were submerged by the noise.

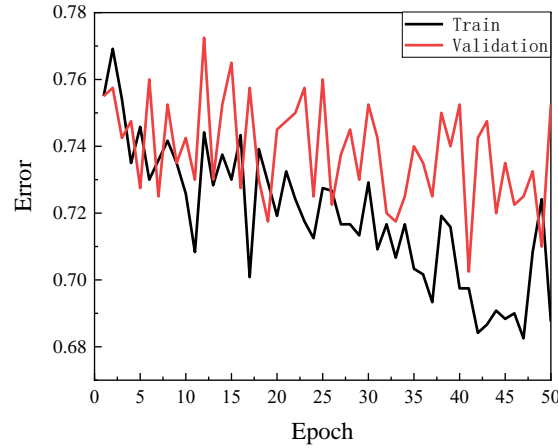


The results of the second network trained by the time-frequency images was shown in **Fig. 5**. Analogically, the training error and validation error spent more time to close to zero when the noise level increased. Under 80 dB, the achieved accuracy was exceptional. The highest accuracies in training and validation was 100% at the third epoch, which increased sharply from 44% and 84% at the first epoch. When the noise level reach to 70 dB, the training and validation error rates were higher, as 0.67 and 0.55 respectively. After training, the error rates dropped down quickly during the first 5 epochs which arrived to 0.17 and 0.14. Then, the rates decreased slowly and were equal to 0.005 and 0.02 at the twentieth epoch. However, the result in 60 dB was not expectable. The two error curves were not converged to zero after 50 epochs' training. The main reason for this should be the input data was hard to identify because of the high noise.



(a) SNR = 80 dB

(b) SNR = 70 dB



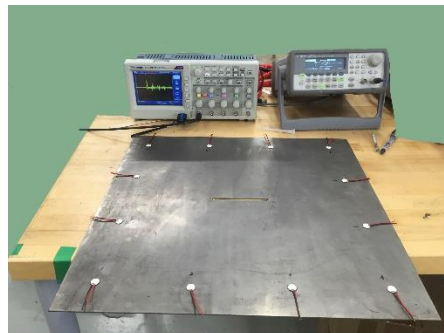
(c) SNR = 60 dB
Fig. 5 Error curve

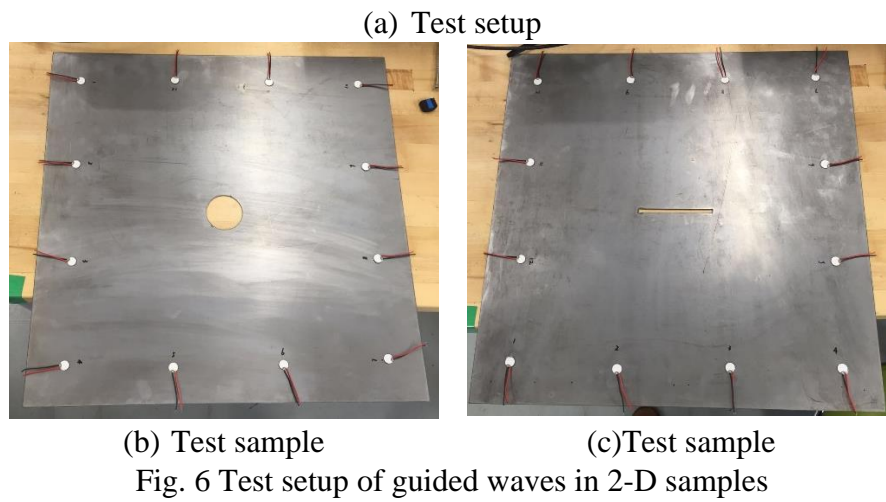
6.4 Data generated from experimental test

6.4.1 Experimental setup

In this section, we attempted to generate data from experimental test, where equipment and environmental noises could be inherent in the measurement. Instead of testing a pipe, we selected 2-dimensional plate as our samples. In the next stage, we planned to select pipe with and without weldment for our case study.

as shown in **Fig. 6**, The experiment consists of generator, oscilloscope, Piezo actuators and a square-shaped steel plate. The actuator array was distributed around the board. The generator submits the voltage signal with different mode. Then actuator changes the voltage signal into mechanical signal. The wave propagates in the steel plate. When it arrives the edge or damage of the steel plate, the signal can be reflected and received by the other actuators. Next, the piezo actuator changes the wave into voltage signal. Two damage types were designed, including a circular damage and a notch-shaped damage.





The dimension of steel plate was 20-inch width, 20-inch long and 1.6 mm thick. Two damages, notch-shaped and circular shaped damage, were designed for this test. 12 actuators were glued on the steel plate, as shown in **Fig. 6**, which included one located at 2 point for inputting the signal and eleven for receiving the signal.

6.4.2 Signal collected from the test

Received signal was shown in **Fig. 7** which contained the 11 received signals in two different damage states. The signals were denoised by wavelet transform method. From the signals, the distinguish between these two damage types were obviously. Adding noise into these signals, the data enlarged in to 500 for each damage type. These data were acted as the input training the CNN for classification.

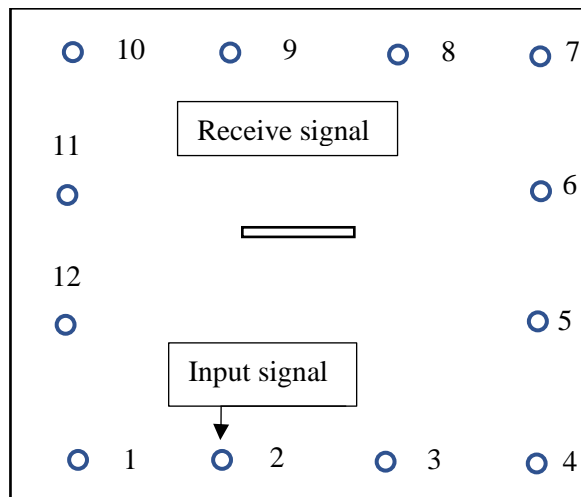
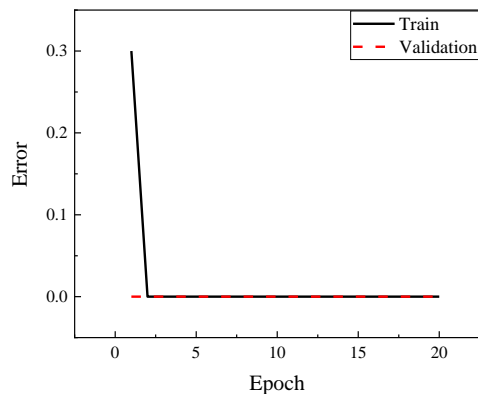
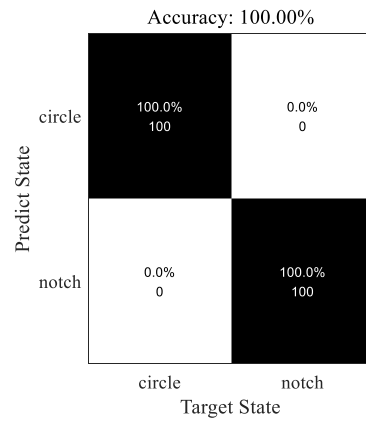


Fig.7 Damage and actuators location in steel plate

The result of the training and validation was shown in **Fig. 8(a)**. The accuracies of classification in training and validation were reach to 100% at the second epoch which means that the signals were easy to be classified. In **Fig. 8(b)**, the result of the testing was also 100% that all the testing samples were classified into the label they belong to.



(a) Error curve



(b) Confusion matrix

Fig. 8 Experiment results

(e) Description of any Problems/Challenges

No problems are experienced during this report period

(f) Planned Activities for the Next Quarter

The planned activities for the next quarter are listed below:

- More experimental and numerical tests for continuing efforts by decoding variance experienced from material and structural integrity.
- Modeling and decoding variance experienced from structural uncertainties.